Radiation Measurements 71 (2014) 518–523

Contents lists available at ScienceDirect

Radiation Measurements

journal homepage: www.elsevier.com/locate/radmeas

Luminescence studies of 100 MeV Si^{8+} ion irradiated nanocrystalline Y_2O_3

N.J. Shivaramu [a], B.N. Lakshminarasappa [a,*], K.R. Nagabhushana [b], Fouran Singh [c]

[a] Department of Physics, Jnanabharathi Campus, Bangalore University, Bangalore 560056, India
[b] Department of Physics (S & H), PES Institute of Technology, 100 Feet Ring Road, Banashankari 3rd Stage, Bangalore 560085, India
[c] Inter University Accelerator Centre, P.O. Box No. 10502, New Delhi 110067, India

HIGHLIGHTS

- Combustion synthesized Y_2O_3 revealed cubic structure.
- 100 MeV Si^{8+} ions doesn't induce phase transition in combustion synthesized Y_2O_3.
- The prominent TL glow peak intensity increases up to 1×10^{11} ions cm^{-2}.
- The experimental TL glow curves revealed second order kinetics.

ARTICLE INFO

Article history:
Available online 13 April 2014

Keywords:
Combustion synthesis
XRD
FTIR
Swift heavy ions
Photoluminescence
Thermoluminescence

ABSTRACT

Combustion synthesized Y_2O_3 revealed cubic structure and the average crystallite size is found to be 32.73 nm. FTIR spectra revealed Y–O, OH stretching and C–O bending bonds. Y_2O_3 pellets are irradiated with 100 MeV Si^{8+} ions in the fluence range 1×10^{10} to 1×10^{14} ions cm^{-2}. PL of irradiated samples shows emission with peaks at 417, 432, 465 nm. Y_2O_3 shows a prominent well resolved TL glow with peak at ~403 K (T_{m1}) and a weak TL peak at 461 K (T_{m2}). TL intensity in the present work increases up to about 1×10^{11} ions cm^{-2} there after it decreases. The TL kinetic parameters are calculated by glow peak shape method. Activation energy and frequency factors are found to in the range of ~1.6 eV and ~10^{18} s^{-1} respectively.

1. Introduction

Yttrium oxide (Y_2O_3) also known as yttria is an important material in many fields such as optics, optoelectronics, radiation dosimetry etc. It is a promising host for high performance composite materials due to its high chemical durability and thermal stability. Y_2O_3 is a rare earth sesquioxide which has been widely used in coating materials and as a red emitting phosphor. (Lin Wang et al., 2009; Akihiro Fukabori et al., 2007). Swift heavy ion (SHI) irradiation induce changes in nano materials in a controlled way and this helps to structure evolution. Energetic heavy ion interacting with material deposits its energy through electronic energy loss (S_e) which is more dominant than nuclear energy loss (S_n). Point defects, defects clusters and ion tracks can be induced in the irradiated materials along the projected range with defect structure depending on the energy loss values and fluences (Yufeng Song et al., 2007). Energetic heavy ions create cylindrical tracks with complex damage structures such as radical formation, intermolecular cross linking, creation of triple bonds etc (Youmei Sun et al., 2003). For such energy loss, the damage process is more complex and the energetic ions deposit extremely high energy to the target. Two different mechanisms namely Coulomb explosion (Fleischer et al., 1965) and thermal spike (Wang et al., 1994) are used to explain the track formation. The Coulomb explosion model is based on the assumption that the intense ionization and excitation along the ion path leads to an unstable zone in which atoms are ejected into the non excited region of the solid by Coulomb repulsion. In thermal spike model, the energy deposited by the ion leads to an increase in transient temperature. The cylindrical volume around the ion path finally reaches the melt phase which is subsequently quenched by thermal conduction (Gamboa-deBuen et al., 1998).

Thermoluminescence (TL) is a well established and very sensitive technique for estimating the concentration of luminescent

* Corresponding author. Tel.: +91 9448116281; fax: +91 80 23219295.
E-mail addresses: bnlnarassappa@rediffmail.com, nagkr@rediffmail.com (B. N. Lakshminarasappa).

http://dx.doi.org/10.1016/j.radmeas.2014.03.027
1350-4487/

centers and nature of traps (defect centers) created in solids. From a practical point of view, the knowledge of the TL response as a function of dose, type of ion and its energy etc permits us for selecting materials for TL dosimeters. (Gamboa-deBuen et al., 1998). The objective of the present work is to study SHI induced luminescence properties of combustion synthesized nanocrystalline yttrium oxide.

2. Material and methods

Nanocrystalline yttrium oxide powder is synthesized by solution combustion technique. Yttrium nitrate hexa hydrate (Sigma Aldrich) and urea (Merck chemicals, India) are used as starting materials. 7.66 g of yttrium nitrate hexa hydrate (oxidizer) and 3.003 g of urea (fuel) are dissolved in a 50 ml of double distilled water in a cylindrical Pyrex dish of 300 ml capacity. This solution is stirred well to ensure homogeneity. The dish containing the homogeneous solution is introduced into a muffle furnace maintained at 500 ± 5°C. Initially, the solution boils and undergoes dehydration followed by decomposition with evaporation of gases leaving behind the powder. To remove the carbon impurities if any left behind, the powder is annealed at 700°C for 2 h (Lakshminarasappa et al., 2012). Pellets of 1 mm thick and 5 mm diameter are prepared by taking 40 mg of Y_2O_3 powder with 4% of Poly vinyl alcohol (PVA) solution (Shibani Das, 2011) and by applying a pressure of 4 MPa using a homemade pellatizer. These pellets are annealed at 900°C for 2 h. Since PVA has low boiling point (228°C) it is not retained in the samples after annealing. The annealed samples are used for irradiation. One of the pellets is used as pristine for comparison with that of irradiated ones. The pellets are irradiated with 100 MeV swift Si^{8+} ions having 2 pnA current (the beam current is 16 nA and charge state of ion is +8) (Nagabhushana ., 2008b). The irradiation fluences are varied from 1×10^{10}–1×10^{14} ions cm^{-2}. This experiment is performed using 16 MV tandem Van de Graff type electrostatic accelerator (15 UD Pelletron) at the Inter University Accelerator Center, New Delhi, India. The full detail of this set up is given elsewhere (Kanjilal et al., 1993). A series of pellets are mounted on a 10 cm length, 2.5 cm width and 2 mm thickness glass slide which in turn mounted on a copper target ladder using double sided tape. The ion beam is magnetically scanned on one cm^2 area on samples surfaces for uniform irradiation. A group of four pellets are irradiated for a particular fluence at a time for TL, PL, XRD and FTIR studies.

Powder X-ray diffraction patterns are recorded using advanced D-8 X-ray diffractometer (Bruker AXS Germany) using 1.5406 Å CuKα radiations. The fourier transform infrared (FTIR) spectra are recorded using a Nicolet spectrometer. Powder from the irradiated surface of pellets is mixed with KBr for FTIR studies. PL emission spectra are recorded using Perkin Elmer LS-55 spectrometer. The samples are excited using a Xenon lamp at 250 nm to record PL emission spectra. TL glow curves are recorded at a heating rate of 5 Ks^{-1} using Harshaw TLD reader (model 3500). The irradiated surface is kept facing towards the detector side in a TLD reader. All experiments are performed at room temperature.

3. Results and discussion

The electronic energy loss, nuclear energy loss and projected ion range (R_p) are calculated from stopping and range of ions in matter (SRIM) software (Ziegler et al., 2010). The ion impact parameters are tabulated in Table 1. SHI irradiation induces phase transformation from cubic to monoclinic structure of yttrium oxide when S_e is 18 keV nm^{-1} (Gaboriaud et al., 2013). In the present work, S_e (4.103 keV nm^{-1}) is much lower than 18 keV nm^{-1}. Hence, phase transformation is not observed instead large numbers of point defects responsible for luminescence are created.

Table 1
Ion impact parameters of Y_2O_3.

Ions	Energy (MeV)	S_e (keV nm^{-1})	S_n (keV nm^{-1})	R_p (μm)	Reference
Au^{8+}	110	21.40	0.406	9.78	Som et al., 2014
Ag^{9+}	120	18.67	0.089	10.87	
Ni^{7+}	150	11.87	0.017	16.68	
Si^{8+}	100	4.103	0.003	21.65	Present work

The XRD patterns of pristine (unirradiated) and SHI irradiated yttrium oxide pellets are shown in Fig. 1a. The XRD pattern

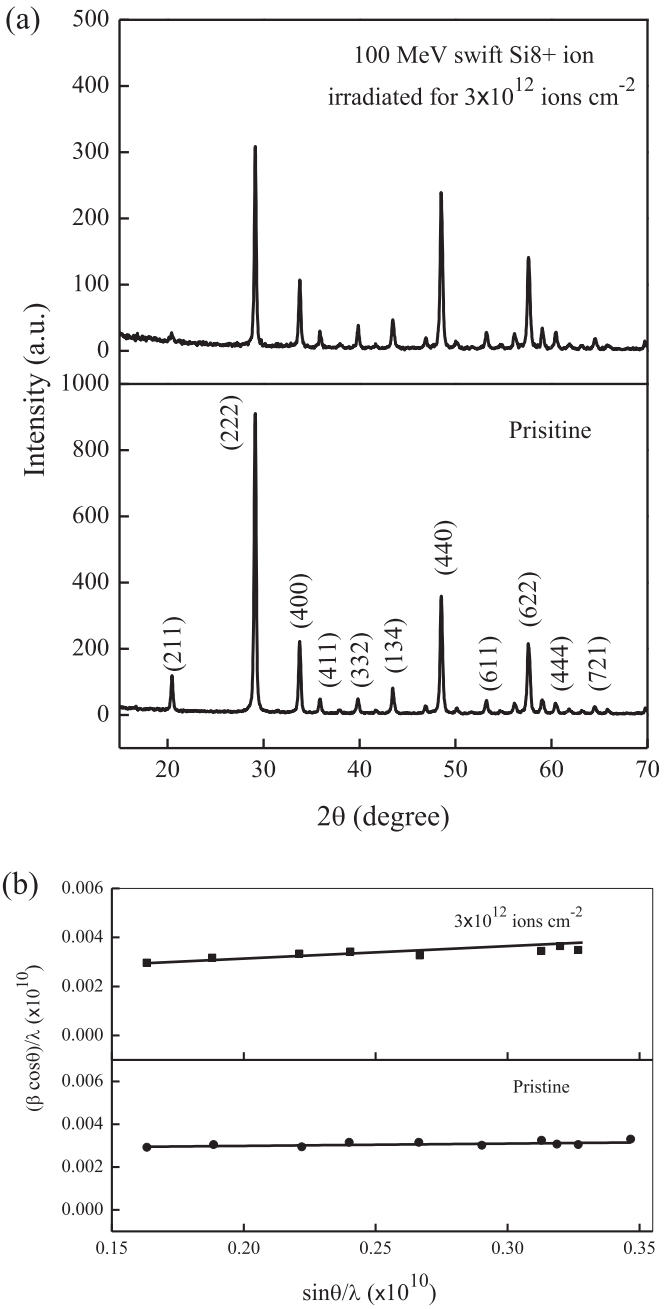

Fig. 1. (a). X-ray diffraction patterns of pristine and 100 MeV swift Si^{8+} ion irradiated Y_2O_3. (b). W–H plot of pristine and 100 MeV swift Si^{8+} ion irradiated Y_2O_3.

Table 2
XRD structural parameters of pristine and 100 MeV swift Si^{8+} irradiated Y_2O_3 (ion fluence: 3×10^{12} ions cm^{-2}).

Samples	Crystallite size D (nm)		Lattice constant a (Å)	Cell volume ($Å^3$)	Density ρ (gm cm^{-3})	Dislocation density δ ($\times 10^{15}$)	Inter-planar space in at (222) (Å)	Lattice strain (%) W–H method
	Scherrer method	W–H method						
Pristine	32.73	37.04	10.590	1187.578	5.053	1.141	3.057	0.025
Irradiated	27.50	33.33	10.603	1192.027	5.033	1.322	3.062	0.063

represents cubic crystal system with space group $1a\bar{3}$. (JCPDS: No: 88-1040; Tong Liu et al., 2012). The structure parameters such as miller indices (hkl), crystallite size (D), inter planar spacing (d), lattice constant (a), cell volume (V), density (D_x), dislocation density (δ) and lattice strain (ε) are calculated from XRD data and tabulated in Table 2. The crystallite size (D) are calculated using Scherrer equation

$$D = \frac{0.9\,\lambda}{\beta \cos\theta} \tag{1}$$

where, λ is the wavelength of X-ray (1.5406 Å), β is full width at half maxima (FWHM) and θ is the Bragg angle. The average crystallite size is found to be 32.73 nm for pristine and 27.50 nm for ion irradiated samples. The phase transformation is not observed in ion irradiated samples. However, the XRD intensity of the irradiated sample is observed to be lower than that of pristine one. This might be due to the creation of large number of defects and discontinuous tracks in sample.

Strain induced broadening arises from crystal imperfections and stress. The lattice strain and crystallite size are estimated using Williamson–Hall (W–H) method following the equation (Khorsand Zak et al., 2011),

$$\frac{\beta\,\mathrm{Cos}\theta}{\lambda} = \frac{1}{D} + \frac{4\varepsilon \mathrm{Sin}\theta}{\lambda} \tag{2}$$

where, ε is the lattice strain. A plot of $(\beta\ \cos\theta)/\lambda$ versus $\sin\theta/\lambda$ is given in Fig. 1(b). Form the plot, the average crystallites size are found to be 37.04 nm for pristine and 33.33 nm for ion irradiated samples. The lattice strain is estimated using W–H plot. It is found to be 0.025% for pristine and 0.063% for irradiated Y_2O_3. The dislocation density is found to be 1.141×10^{15} m^{-2} for pristine and 1.32×10^{15} m^{-2} for irradiated samples. The increase in ε and δ in irradiated samples might be due to extended defects created in the material. Further, ε is found to be positive for both samples (Khorsand Zak et al., 2011).

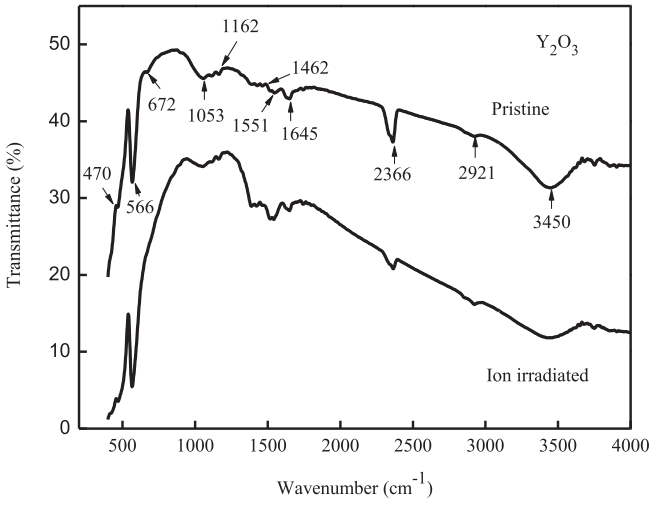

Fig. 2. FTIR spectra of pristine and 100 MeV swift Si^{8+} ion irradiated Y_2O_3 (Ion fluence: 3×10^{12} ions cm^{-2}).

FTIR spectra of pure and irradiated (3×10^{12} ions cm^{-2}) Y_2O_3 are shown in Fig. 2. The vibrational bands at 470, 566, 672, 1053, 1162, 1462, 1551, 1645, 2921 and 3450 cm^{-1} are observed in both samples. The band at 2366 cm^{-1} is attributed to C=O bond (Faheem Ahmed et al., 2012). The bands at 470 and 566 cm^{-1} are due to Y–O stretching vibrations. The bands at 672, 1053 and 1162 cm^{-1} are ascribed to C–O bending and bands at 1462, 1551 and 1645 cm^{-1} are attributed to C–O Stretching vibrations (Som et al., 2014; Lakshminarasappa et al., 2012). The bands at 1645, 2921 and 3450 cm^{-1} are well known and assigned to OH stretching vibrations (Magalaraja et al., 2009). The carbon bonds appeared in the FTIR spectra are due to trace impurities left during by the fuel used in the synthesis. FTIR spectrum gives the vibration of bonds in a given system. The vibrational bond depends on starting ingredients, annealing condition, spectra recording condition etc. It is found that the intensity of vibrational modes is lower in irradiated samples. This indicates that the bonds responsible for FTIR modes are broken due to large amount of energy deposited through S_e. The FTIR vibrational bands and intensities with their assignments are given in Table 3.

Photoluminescence (PL) is a well established, nondestructive and widely practiced tool for the identification of defects in opaque materials where optical absorption studies cannot be carried out. Therefore, PL is used as a technique to identify the ion induced defects. Fig. 3 (a) shows PL spectra of pristine and 100 MeV swift Si^{8+} ion irradiated yttrium oxide samples. Sharp PL emissions with peak at 417, 432 and 465 nm are observed in both pristine as well as ion irradiated samples. Bordun (2002) studied the influence of oxygen vacancies on luminescence spectra of Y_2O_3. He concluded that the luminescence bands with maxima at 365 and 428 nm are due to presence of oxygen vacancies related to radiative recombination. Osipov and coworkers studied luminescence of pure yttria (Osipov et al., 2008). They reported cathodoluminescence spectra with peak at 465 nm and the emission is ascribed to recombination of associative Y^{3+}–O^{2-} donor acceptor pair. The reported

Table 3
FTIR absorption peaks of pristine and 100 MeV swift Si^{8+} irradiated (ion fluence: 3×10^{12} ions cm^{-2}).

FTIR absorption peaks (cm^{-1})				
Pristine	Normalized peak height (a.u.)	Irradiated	Normalized peak height (a.u.)	Modes
470	0.20	470	0.16	Y–O Stretching
566	9.64	566	9.42	Y–O Stretching
672	0.39	672	–	C–O bending
1053	0.44	1046	0.32	C–O bending
1162	0.33	1162	0.30	C–O bending
1462	0.31	1462	0.28	C–O Stretching
1551	0.32	1551	0.25	C–O Stretching
1645	1.28	1645	2.04	–OH Stretching
2366	3.65	2366	1.17	C=O stretching
2921	0.22	2921	0.14	–OH Stretching
3450	4.03	3450	1.99	–OH Stretching

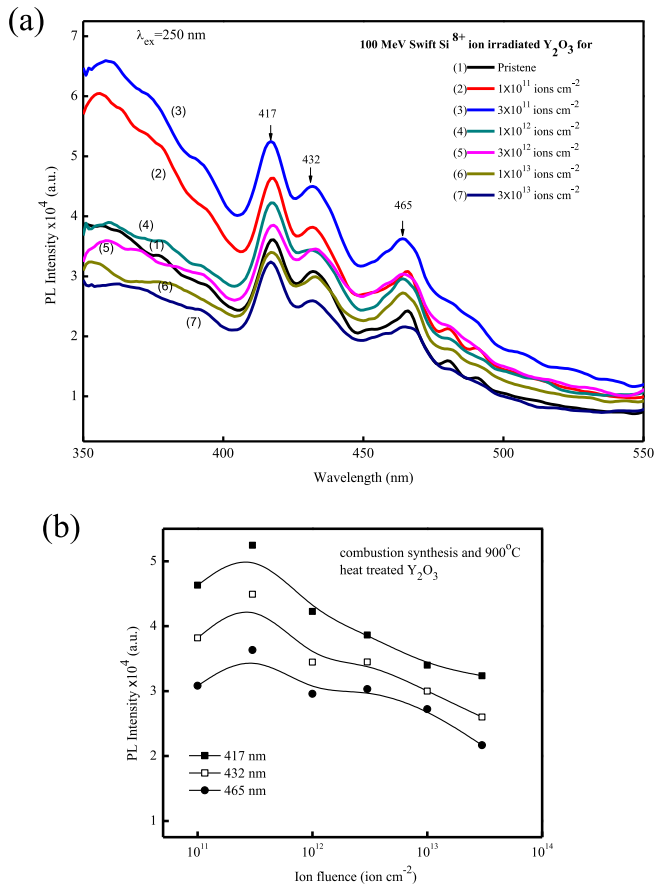

Fig. 3. (a). Photoluminescence spectra of pristine and 100 MeV swift Si^{8+} ion irradiated Y_2O_3. (b). Variation of PL intensity with ion fluence in SHI irradiated nanocrystalline Y_2O_3.

luminescence bands with peaks at 428 and 465 nm are matching with the present work. The PL emission with peaks at 417 and 432 are attributed to oxygen vacancy defects such as F and F^+-centers (Nagabhushana et al., 2007; K.S. Jheeta et al., 2006) and 465 nm is attributed to Y^{3+}–O^{2-} donor acceptor pair.

Fig. 3(b) shows variation of PL intensitiy as a function of ion fluence in Y_2O_3. The PL intensity at 417, 432 and 465 nm peaks is found to increase with increase in ion fluence up to 3×10^{11} ions cm^{-2} and then decreases with further increase in ion fluence. At higher fluences the decrease in PL intensity might be due to the destruction of defects. The defects might be annihilated and/or transformed in to complex centers and change in the energy levels of the crystal resulting from the perturbation of the luminescent sites during the ion irradiation process (Gaboriaud et al., 2013; Nagabhushana et al., 2006).

Fig. 4 (a) shows TL glow curves of 100 MeV swift Si^{8+} ion irradiated combustion synthesized yttrium oxide for various fluence. A prominent and well resolved TL glow with peak at ~403 K (T_{m1}) is observed along with a weak TL glow with peak at 461 K in all irradiated samples. Som and co workers investigated the TL response of combustion synthesized Y_2O_3:Tb^{3+} nanophosphor irradiated with 150 MeV Ni^{7+}, 120 MeV Ag^{9+} and 110 MeV Au^{8+} ions. A prominent TL glow with peak at 585, 605 and 630 K are reported in Au, Ag and Ni ion irradiated samples (Som et al., 2014) respectively. They observed that TL intensity increases with increase in ion fluence up to 1×10^{12} ions cm^{-2} for Ni and Ag ions. And, in the case of Au ions the TL intensity is linear in the study range. The TL glow peak temperature shifts towards lower temperature region with increase in Z-number of ion species used for irradiation. The ion impact parameters of Ni, Ag and Au ions are compared with Si ion and given in Table 1. The TL intensity of the ion induced nanomaterials is found to decrease while going from low atomic number to high atomic numbers ions (Numan salah et al., 2007). Hence, we performed the irradiation with Si ions. Som (Som et al., 2014) reported high temperature TL glows in ion irradiated samples and these peaks might be due to Tb^{3+} emission centers. Som concluded that loss of crystallinity is more in Au^{8+}ion irradiated phosphors where S_e is 21.40 keV nm^{-1}. Since Si is a low Z ion when compared to Au, Ag and Ni, the S_e is 4.126 keV nm^{-1} on the samples the loss of crystallinity is small. This is confirmed by from XRD results. Hence, in the present work the TL glow peak is attributed to SHI induced intrinsic defects F and F^+ centers.

Fig. 4 (b) shows the variation of prominent TL glow peak intensity (I_{m1}) and glow peak temperature (T_{m1}) with ion fluence. It is observed that the glow peak intensity increases up to a fluence of 1×10^{11} ions cm^{-2} then it decreases with further increase of ion fluence. The increase is TL intensity indicates the increase of luminescence centers (LCs) are created up to a fluence of 1×10^{11} ions cm^{-2} and then it reaches the saturation level with further increase in ion fluence. This can be explained by the track interaction model (Szenes, 1999; Som et al., 2014). According to this model at low fluence, electrons escaping from the ion tracks are recombining with the nonradiative centers in the intermediate region. The TL signal is proportional to the number of ion tracks.

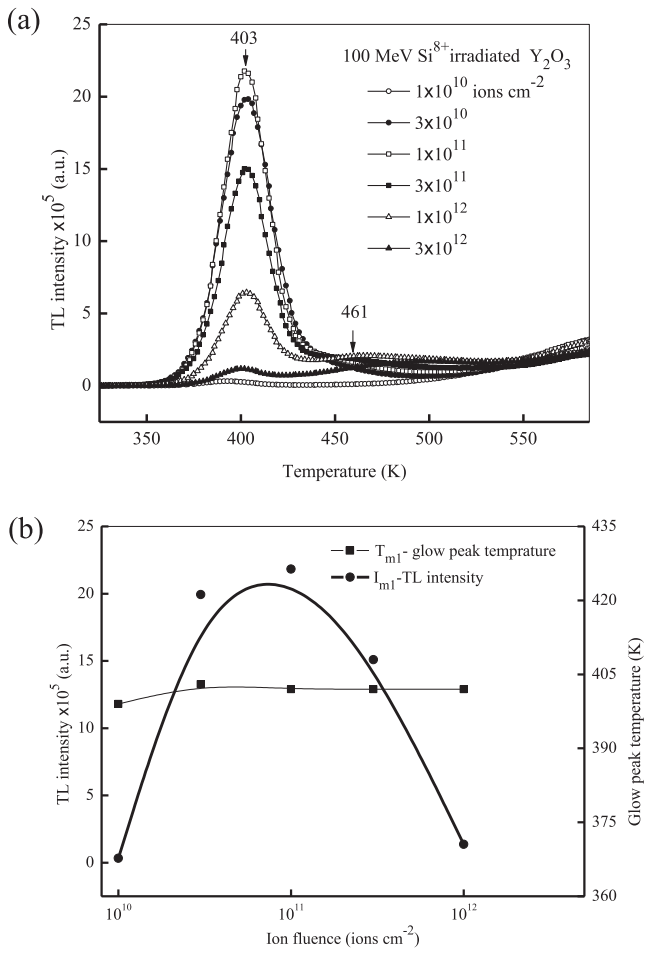

Fig. 4. (a). Thermoluminescence glow curves of 100 MeV swift Si^{8+} ion irradiated nanocrystalline Y_2O_3. (b). Variation of TL glow peak (I_m) intensity and glow peak temperature (T_m) with ion fluences in irradiated nanocrystalline Y_2O_3.

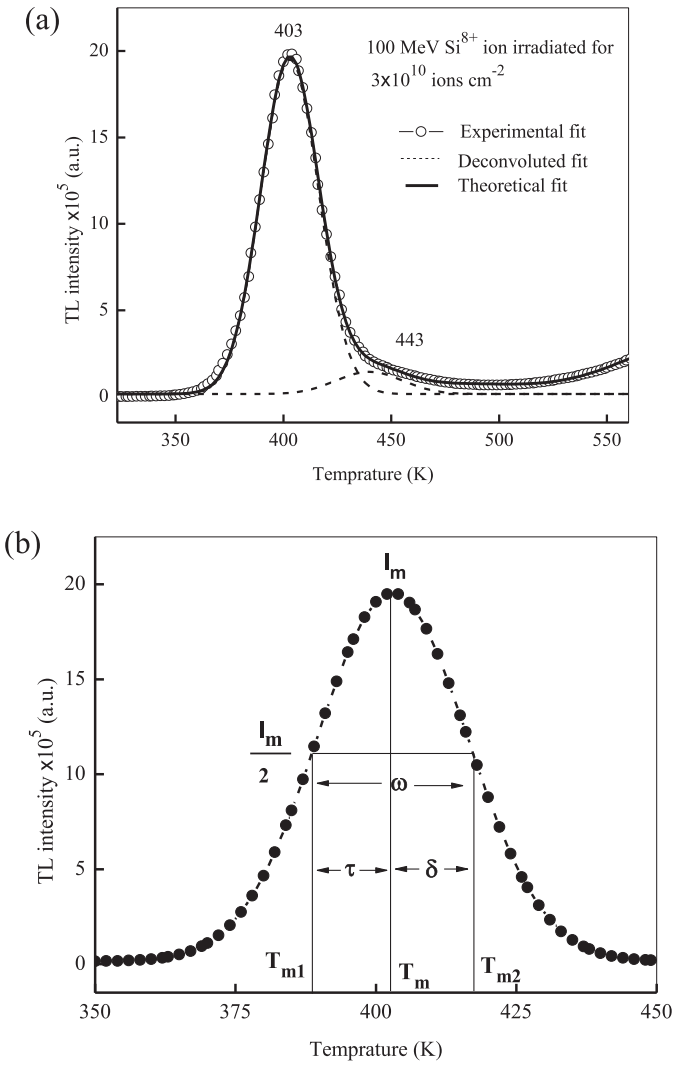

Fig. 5. (a). Deconvoluted TL glow curve of 100 MeV swift Si^{8+} ion irradiated nanocrystalline Y_2O_3 (Ion fluence: 3×10^{10} ions cm^{-2}). (b). Parameters used in the glow curve shape method (modified by Chen).

Further increasing ion fluence/dose, the separation between ion tracks is reduced. Therefore, effective electrons escaping from tracks is more and more escaping electrons recombine with positive centers resulting in more TL signal with further increasing ion fluence the tracks overlap each other and effective escaping electrons reduced, resulting in decreased TL signal (Numan salah et al., 2007).

Estimation of the kinetic parameters such as activation energy (E) of the traps involved in TL emission, order of kinetics (b), frequency factor (s) and trap density (n_o) associated with the TL glow peaks are quite informative on the nature of defect center created. Fig. 5(a) shows a typical deconvoluted TL glow curves of 100 MeV swift Si^{8+} ions for the fluence 3×10^{10} ions cm^{-2}. The experimentally recorded glow curve is deconvoluted in to two TL glows with peak at 403 and 443 K. The theoretically obtained TL glow curves are fitted with the experimental data and the quality of fitting is described by figure of merit (FOM). The fits are considered to be adequate when the FOM values are below 5% (Som et al., 2014). The FOM for the present curve fitting is 3.2% which indicates that a good agreement between theoretically generated and experimentally recorded TL glow curves. The trap parameters of TL curves are calculated using the glow curve shape method (modified by Chen). The equations involved in these calculations are given elsewhere (Nagabhushana et al., 2008). The parameters τ, δ, and ω extracted from TL glow curve as shown in Fig. 5(b). The trap density is calculated using the following relation (Suriyamurthy and Panigrahi, 2008).

$$n_o = \frac{\omega I_m}{\beta\left\{2.52 + 10.2\left(\mu_g - 0.42\right)\right\}} \quad (3)$$

The value of geometry factor (μ_g), 0.42 and 0.52 typically represents first and second order kinetics respectively. In the present work, μ_g is found to be 0.50 to 0.52 and this implies that glow curves indicates the second order kinetics. The kinetic parameters are given in Table 4.

Numan salah studied Li ion irradiated TL and PL of $LiNaSO_4$ nanoparticles. They reported the frequency factor of 1.6×10^{21} s^{-1} (Numan Salah et al., 2006). Manjunatha reported the frequency factor in the magnitude of $\sim10^{20}$ and $\sim10^{13}$ s^{-1} for Si ion irradiated and UV irradiated $CdSiO_3$ nanophosphors respectively (Manjunatha et al., 2013). Lakshminarasappa et al. (2012) reported the TL of γ-irradiated Y_2O_3 and the trap parameters are reported to be 0.7 eV and 0.23×10^{9} s^{-1} for 610 K peak. In the present work, activation energy and frequency factor are observed to be ~1.6 eV and $\sim10^{18}$ s^{-1} respectively. TL trap parameters depend on synthesis method, annealing procedure, nature of exposing radiation, energy, dose/fluence rate, nature of sample, heating rate, sensitivity of TL reader, atmosphere conditions etc. Also, it is expected that under high energy ion irradiation, TL glow curve structure might be changed because of the TL trapping and recombination mechanism are sensitive to any perturbation. Hence, kinetic parameters may not be directly related to physical process such as lattice vibrational frequencies (Yang et al., 2002; Benyagoub et al., 2001). Moreover, the uncertainty in the frequency factor may also due to in homogeneity of the ion beam, sensitivity difference of the samples and uncertainties in curve fitting. Therefore, in the present work, TL

Table 4
TL kinetic parameters of 100 MeV swift Si^{8+} irradiated Y_2O_3.

Ion fluence (ions cm^{-2})	T_m (K)	μ_g	b	E_τ (eV)	E_δ (eV)	E_ω (eV)	E_{av} (eV)	s (s^{-1})	$n_o \times 10^5$ (cm^{-3})
1×10^{10}	399	0.50	2	1.07	1.07	0.91	1.00	1.59×10^{12}	0.79
	442	0.48	2	1.04	1.07	0.91	1.00	1.57×10^{6}	0.25
3×10^{10}	403	0.48	2	1.36	1.35	1.36	1.36	4.49×10^{16}	38.36
	443	0.48	2	1.21	1.23	1.07	1.17	6.68×10^{12}	3.85
1×10^{11}	402	0.51	2	1.79	1.69	1.57	1.68	8.69×10^{20}	29.70
	450	0.50	2	0.87	0.91	0.71	0.83	4.53×10^{8}	7.55
3×10^{11}	402	0.51	2	1.79	1.68	1.57	1.68	8.69×10^{20}	20.70
	458	0.49	2	0.67	0.74	0.53	0.65	2.27×10^{8}	0.77
1×10^{12}	403	0.50	2	1.56	1.53	1.40	1.38	9.50×10^{16}	10.17
	461	0.48	2	0.49	0.57	0.49	0.52	6.47×10^{4}	12.30

glow curves and traps parameters are different than previously reported ones.

4. Conclusions

Pure nanocrystalline Y_2O_3 phosphors synthesized by combustion technique show cubic structure. Lattice strain and dislocation density are having higher value due to extended defects created by SHI irradiation. Phase transformation from cubic to monoclinic structure of yttrium oxide is not induced by 100 MeV swift Si^{8+} ions. FTIR spectra confirmed the destruction of C–O bending after SHI irradiation. PL emissions at 417 and 432 nm are due to F and F^+-centers and 465 nm is due to Y^{3+}–O^{2-} donor–acceptor pair. Intensity of prominent TL glow at 403 K increases up to a fluence of 1×10^{11} ions cm^{-2}. Effective electrons escaping from tracks is higher resulting in more TL signal. Beyond this fluence the TL intensity reduces due to lack of recombination centers. The TL glow curves exhibit second order kinetics. Since, the Si ion irradiated nanocrystalline Y_2O_3 exhibits TL glow in lower temperature region the material can be tested for its dosimetric properties viz fading, energy response, sensitivity, reproducibility and recycling tests.

Acknowledgments

The authors express their sincere thanks to Dr. D.K. Avasthi, Materials Science Group, Dr. S.P. Lochab, Health Physics Group, Inter University Accelerator Centre, New Delhi, India for their constant encouragement and help during the experiment. Also, one of the authors (NJS) is grateful to Inter University Accelerator Centre, New Delhi, for providing fellowship under UFR (No. 48303) scheme.

References

Ahmed, Faheem, Kumar, Shalendra, Arshi, Nishat, Anwar, M.S., Koo, Bon Heun, Lee, Chan Gyu, 2012. Doping effects of Co^{2+} ions on structural and magnetic properties of ZnO nanoparticles. Microelectron. Eng. 89, 129–132.

Benyagoub, A., Couvreur, F., Bouffard, S., Levesque, F., Dufour, C., Paumier, E., 2001. Phase transformation induced in pure zirconia by high energy heavy ion irradiation. Nucl. Instrum. Methods Phys. Res. B 175, 417–421.

Bordun, O.M., 2002. influence of oxygen vacancies on the luminescence spectra of Y_2O_3 thin films. J.Appl. Spectr. 69, 430–433.

Das, Shibani, 2011. Study of Composition Behavior of Binders and the Effect of Bender Type on Strength and Density of Alumina Samples‖. Thesis. B.Tec, National institute of Technology Rourkela, pp. 26–27. Chapter 3.

Fleischer, R.L., Price, P.B., Walker, R.M., 1965. Ion explosion spike mechanism for formation of charged particle tracks in solids. J. Appl. Phys. 36, 3645.

Fukabori, Akihiro, Sekita, Masami, Ikegami, Takayasu, Iyi, Nobuo, Komatsu, Toshiki, 2007. Induced emission cross section of a possible laser line in Nd: Y_2O_3 ceramics at 1.095 m. J. Appl. Phys. 101, 043112.

Gaboriaud, R.J., Paumier, F., Jublot, M., Lacroix, B., 2013. Ion irradiation-induced phase transformation mechanisms in Y_2O_3 thin films. Nucl. Instrum. Methods Phys. Res. B 311, 86–92.

Gamboa-deBuen, Ruiz, C., Oliver, A., Lopez, K., Brandan, M.E., 1998. Measurement of the thermoluminescent response (supralinearity and efficiency) of LiF: mg,Ti exposed to 0.7 MeV Protons. Nucl. Instrum. Methods Phys. Res. B 134, 136–148.

Jheeta, K.S., Jain, D.C., Kumar, Ravi, Singh, Fouran, Garg, K.B., 2006. Photoluminescence study of swift heavy ion (SHI) induced defect centers in sapphire. J. Nucl. Mater. 353, 190–192.

Kanjilal, D., Chopra, S., Narayanan, M.M., Iyer Indira, S., Vandana, R.J.J., Datta, S.K., 1993. Testing and operation of the 15UD Pelletron at NSC. Nucl. Instrum. Methods Phys. Res. A 328, 97–100.

Khorsand Zak, Abd Majid, W.H., Abrishami, M.E., Yousefi, Ramin, 2011. X-ray analysis of ZnO nanoparticles by Williamson–Hall and size–strain plot methods. Solid State Sci. 13, 251–256.

Lakshminarasappa, B.N., Jayaramaiah, J.R., Nagabhushana, B.M., 2012. Thermoluminescence of combustion synthesized yttrium oxide. Powder Technol. 217, 7–10.

Liu, Tong, Xu, Wen, Bai, Xue, Song, Hongwei, 2012. Tunable silica shell and its modification on photoluminescent properties of Y_2O_3:Eu^{3+}@SiO_2 nanocomposites. J. Appl. Phys. 111, 064312.

Mangalaraja, R.V., Mouzon, J., Hedstrom, P., Camurri, Carlos P., Ananthakumar, S., Oden, M., 2009. Microwave assisted combustion synthesis of nanocrystalline yttria and its powder characteristics. Powder Tech. 191, 309–314.

Manjunatha, C., Sunitha, D.V., Nagabhushana, H., Singh, Fouran, Sharma, S.C., Chakradhar, R.P.S., Nagabhushana, B.M., 2013. Thermoluminescence properties of 100 MeV Si7+ swift heavy ions and UV irradiated $CdSiO_3$:Ce^{3+} nanophosphor. J. Lumin. 134, 358–368.

Nagabhushana, K.R., 2008. Thermoluminescence and Photoluminescence Studies in Swift Heavy Ion Irradiated Nanocrystalline Aluminum Oxide. Ph.D Thesis. Bangalore University, p. 44. Chapter 2.

Nagabhushana, H., Lakshminarasappa, B.N., Prashantha, S.C., Nagabhushana, K.R., Singh, Fouran, 2006. Spectroscopic studies of swift heavy ion irradiated nanophase mullite. Nucl. Instrum. Methods Phys. Res. B 244, 31–33.

Nagabhushana, K.R., Lakshminarasappa, B.N., Chadrappa, G.T., Haranath, D., singh, Fouran, 2007. Swift heavy ion induced photoluminescence studies in aluminum oxide. Radi. Effe. Def. solids 162, 325–332.

Nagabhushana, K.R., Lakshminarasappa, B.N., Singh, Fouran, 2008. Thermoluminescence studies in swift heavy ion irradiated aluminum oxide. Radiat. Meas. 43, S651–S655.

Osipov, V.V., Rasuleva, A.V., Solomonov, V.I., 2008. Luminescence of pure yttria. Opt. Spectrosc. 105, 524–530.

Salah, Numan, Sahare, P.D., Prasad, Awadhesh, 2006. Thermoluminescence and photoluminescence of $LiNaSO_4$:Eu irradiated with 24 and 48MeV ^{7}Li ion beam. J. Lumin. 121, 497–506.

Salah, Numan, Lochab, S.P., Kanjilal, D., Ranjan, Ranju, Habib, Sami S., Rupasov, A.A., Aleynikov, V.E., 2007. Nanoparticles of $K_2Ca_2(SO_4)_3$:Eu as effective detectors for swift heavy ions. J.Appl. Phys. 102, 064904.

Som, S., Dutta, S., Chowdhury, M., Kumar, Vijay, Kumar, Vinod, Swart, H.C., Sharma, S.K., 2014. A comparative investigation on ion impact parameters and TL response of Y_2O_3:Tb^{3+} nanophosphor exposed to swift heavy ions for space dosimetry. J. Alloys Compd. 589, 5–18.

Song, Yufeng, Liu, Qi, Sun, Youmei, Liu, Jie, Zhu, Zhiyong, 2007. Color center formation in α-Al_2O_3 induced by high energy heavy ions. Nucl. Instrum. Methods Phys. Res. B 254, 268–272.

Sun, Youmei, Zhu, Zhiyong, Wang, Zhiguang, Liu, Jie, Jin, Yunfan, Hou, Mingdong, Wang, Ying, Duan, Jinglai, 2003. The damage process induced by swift heavy ion in polycarbonate. Nucl. Instrum. Methods Phys. Res. B 212, 211–215.

Suriyamurthy, N., Panigrahi, B.S., 2008. Effects of non-stoichiometry and substitution on photoluminescence and afterglow luminescence of $Sr_4Al_{14}O_{25}$:Eu^{2+}, Dy^{3+} phosphor. J. Lumin 128, 1809–1814.

Szenes, G., 1999. Amorphous tracks in insulators induced by monoatomic and cluster ions. Phys. Rev. B 60, 3140–3147.

Wang, Z.G., Dufour, C., Paumier, E., Toulemonde, M., 1994. The S_e sensitivity of metals under swift-heavy-ion irradiation: a transient thermal process. J. Phys. Condens. Matter 6, 6733–6750.

Wang, Lin, Pan, Yuexiao, Ding, Yang, Yang, Wenge, Mao, Wendy L., Sinogeikin, Stanislav V., Meng, Yue, Shen, Guoyin, Mao, Ho-kwang, 2009. High-pressure induced phase transitions of Y_2O_3 and Y_2O_3: Eu^{3+}. Appl. Phys. Lett. 94, 061921–061923.

Yang, B., Xie, L., Xu, Y., Townsend, P.D., 2002. Studies on the 30–300 °C thermoluminescence spectra of 3.1 MeV ion beam bombarded LiF: mg, Cu, P. Nucl. Instrum. Methods Phys. Res. B 187, 408–418.

Ziegler, J.F., Ziegler, M.D., Biersack, J.P., 2010. SRIM – the stopping and Range of Ions in Matter. Nucl. Instrum. Methods Phys. Res. B 268, 1818–1823.